Advances in the Analysis and Design of Constant-Torque Springs

John R. McGuire* and Joseph A. Yura**

Abstract

In order to improve the design procedure of constant-torque springs used in aerospace applications, several new analysis techniques have been developed. These techniques make it possible to accurately construct a torque-rotation curve for any general constant-torque spring configuration. These new techniques allow for friction in the system to be included in the analysis, an area of analysis that has heretofore been unexplored. The new analysis techniques also include solutions for the deflected shape of the spring as well as solutions for drum and roller support reaction forces. A design procedure incorporating these new capabilities is presented.

Introduction

Within the aerospace industry the constant-torque spring fulfills an important role. Many spacecraft, such as earth orbiting satellites and interplanetary explorers, once separated from a launch vehicle, must deploy several appendages, such as solar array panels, antennas, and sensory devices. The multi-layered constant-torque spring is often used as a power source to do this (Figures 1 and 2).
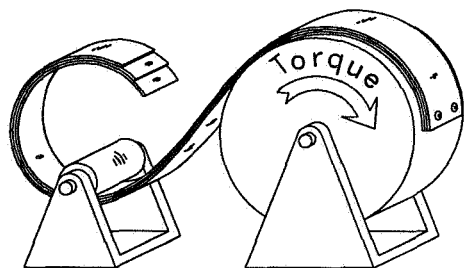
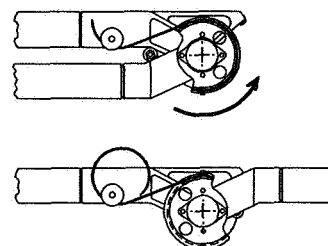**Figure 1. Layered Constant-Torque Spring**

Figure 2. Typical 180° Hinge

The reason for its preference over other power sources includes the fact that the constant torque characteristic satisfies torque requirements over the entire deflection range, while at the same time minimizing the energy to be damped, also the constant-torque characteristic simplifies modeling of the system.

Current Design Difficulties

Although the constant-torque spring is widely used, current analysis and design procedures are restrictive and inefficient. Design charts are provided by spring manufacturers for a finite number of "set" configurations. However, if the engineer

*NASA - Goddard Space Flight Center, Greenbelt, MD
**The University of Texas at Austin, Austin, TX

wishes to deviate from the limited selection, very little about the behavior of the spring can be predicted. Typically, adequate information about the behavior of the spring is not known until after tests are performed to determine the spring's behavior. This results in a time consuming trial and error design process.

To efficiently design a constant-torque spring, the torque-rotation response of the spring throughout the entire range of rotation must be accurately known. Figure 3 shows a typical torque-rotation response curve. The constant portion of the curve can be described using four basic parameters. The constant or average torque value T, the amount of hysteresis due to friction in the system e, the rotation required to develop the full resistance of the spring θ_p, and the maximum or final rotation at which the spring would slip off the roller θ_f.
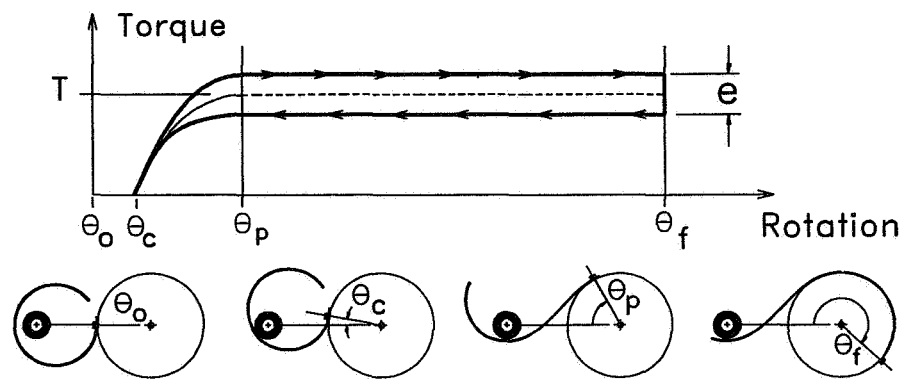

Figure 3. Typical Torque-Rotation Curve

In the past, the only parameter that could be accurately predicted for any general spring configuration was T (Reference 1). There were no analytical methods available for calculating e, θ_p, or θ_f for the general case.

The inability to accurately predict the torque-rotation curve has led to difficulties. For example, the magnitude of the hysteresis in the system is generally unknown. If e can not be estimated analytically, a trial and error design procedure is required in order to optimize the performance of the spring.

In the case shown in Figure 4, the drum size was decreased due to operating space considerations. Since the ratio of drum size to spring size deviates from standard published design charts, no information was available as to the minimum rotation (θ_p) required to develop the full operating torque and could only be confirmed by testing after fabrication of the mechanism. If θ_p could have been determined analytically the testing could have been eliminated or at least reduced.

In the past there have also been no methods available for calculating the deflected shape of the spring. In many cases it is quite advantageous to know the deflected shape and position of the spring. First, calculating the shape of the deflection curve is
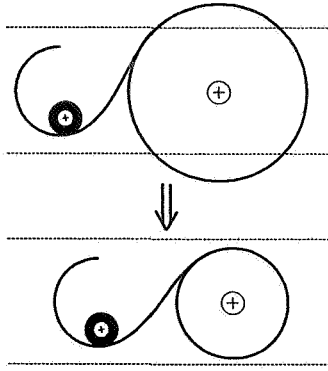
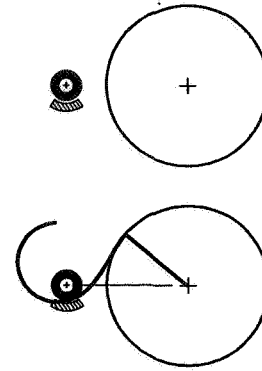**Figure 4. Non-Standard Ratio of Drum Diameter to Spring Diameter**

Figure 5. Guard-Rail Interferes with Spring

advantageous because the exact length of the spring can be determined; there are also other subtle advantages. Figure 5 shows a configuration that was designed with a roller-guard to protect the spring. Since the deflected shape of the spring was unknown, the roller-guard was placed in the most logical position, directly under the roller. However, after the system was assembled it became apparent that the deflected shape of the spring was different than assumed and that the roller-guard would interfere with the spring. This resulted in a trial and error design process.

Testing Program

In order to develop analysis and design techniques so that problems similar to those mentioned above can be avoided an experimental program investigating several aspects of the behavior of the constant-torque spring was carried out at NASA's Goddard Space Flight Center and at The University of Texas at Austin. The results of these tests have led to the development of analysis procedures for completely defining the torque-rotation response of a constant-torque spring, including the effects of friction. Furthermore, the differential equation describing the deflected shape of the spring has been solved for, making it possible to describe the shape of the spring in the loaded configuration and possible to determine the support reaction forces created by the spring. Results will be presented herein that show that the methods developed accurately describe the deflected shape of the spring, and accurately predict the important parameters necessary for constructing the torque-rotation curve.

Definitions and Assumptions

The geometry of the spring coil is uniquely defined by the following fundamental parameters: the width of the spring b, the thickness of the spring t, the natural radius of the spring R_n, the length of the spring S, and in the case of a multi-layered spring, the number of spring layers n (Figure 6). The drum-roller configuration, as shown in Figure 7, consists of the radius of the drum R_d, the radius of the roller R_r, the distance between the center of the drum and the center of the roller L, and the rotation of the

Table 1. Summary of System Parameters and Symbols Used

| Spring Fundamental Geometry	Spring Material and Section Properties
Spring width (b) Spring thickness (t) Spring natural radius (R_n) Spring length (S) Number of spring layers (n)	Young's modulus (E) Yield Strength (σ_y) Bending stiffness (I) $I = bt^3/12$
Drum-roller Fundamental Geometry Drum radius (R_d) Roller radius (R_r) Drum to roller dist (L) Drum rotation (θ)	**Miscellaneous Parameters** Roller coefficient of friction (f)
Secondary Geometric Parameters Spring Initial Diameter (ID) $ID = 2R_n$ Spring natural curvature (ϕ_n) $\phi_n = 1/R_n$ Spring thickness to width ratio (b/t) Spring curvature ratio (β) $\beta = 2R_n/t$ Spring to drum ratio (α) $\alpha = R_d/R_n$	**Geometric Assumptions** Spring width is constant Spring thickness is constant Spring natural radius is constant All spring layers are uniformly shaped Drum is circular and rotates about its center
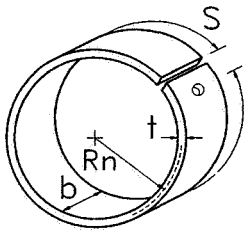
Figure 6. Geometrical Parameters of the Spring Coil
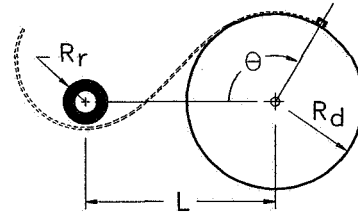

Figure 7. Geometrical Parameters of the Drum and Roller

drum θ. These parameters alone uniquely define the drum roller configuration. Definitions of other parameters and symbols are summarized in Table 1.

The Deflected Shape of the Spring

In this section equations which describe the deflected shape of the spring are presented and two numerical methods for calculating the deflected shape of the spring are proposed. Results using these methods are then compared to test results from the experimental program.

The deformed shape of the loaded spring will be described as a function. Therefore it is necessary to select a coordinate system that allows for only a single value of y for each value of x. It is also advantageous to select a coordinate system that allows for as many initial and final values as possible to be defined. For this purpose the coordinate system shown in Figure 8 was selected. The portion of the spring for which the deflected shape is unknown is that segment between point A, the point were the

spring touches the roller, and point B, the point were the spring becomes tangent to the drum. This is the segment for which the deflection curve must be solved.

Initial values at A
$y(0) = -R_r$
$\theta(0) = 0$
$\phi(0) = 1/R_n$

Final values at B
$y(x_t) = $ unknown
$\theta(x_t) = $ unknown
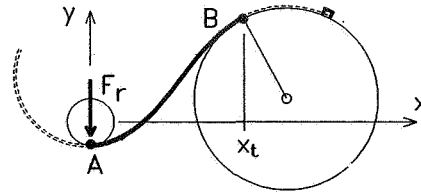$\phi(x_t) = -1/R_d$

Figure 8. Coordinate System

The origin of the coordinate system is the center of the roller. The angular orientation of the coordinate system is not referenced to the drum, but to the roller reaction force F_r. This means that the location of point B and the location of the center of the drum will be unknown. Since F_r must always pass through the center of the roller, F_r will always be collinear with the y axis. Therefore point A will always be at x = 0, and F_r will always be perpendicular to the spring at point A. This is advantageous because the bending moment M at any point along the spring can be simply expressed as the product of F_r and the x coordinate of the point of interest (M = F_r x). This will be true regardless of the effects of large deflections. The change in curvature of the deflection curve is related to the magnitude of the bending moment (M = $\Delta\phi$ EI). Using these relationships it can be shown that the curvature, slope, and deflection at any point along the curve can be expressed using Equations 1, 2, and 3 respectively (Reference 2).

$$\textit{Curvature} \qquad \phi = \phi_n - \frac{F_r x}{EI} \qquad\qquad (1)$$

$$\textit{Slope} \qquad \theta = \sin^{-1}\left[\phi_n x - \frac{F_r x^2}{2EI} \right] \qquad\qquad (2)$$

$$\textit{Deflection} \qquad y = \int_0^x \tan\left[\sin^{-1}\left(\phi_n x - \frac{F_r x^2}{2EI} \right) \right] dx \qquad\qquad (3)$$

It should be noted that the curvature at point B is negative and is equal in magnitude to the curvature of the surface of the drum. Therefore, substituting $-1/R_d$ for ϕ in Equation 1 results in the following expression for x_t.

$$x_t = \left(\frac{1}{R_n} + \frac{1}{R_d} \right) \frac{EI}{F_r} \qquad\qquad (4)$$

Equation 3 is the expression that describes the deflected shape of the spring. Because

there is not a closed form solution for the integral expression, numerical calculation of the integral is required. Furthermore, because the reaction force F_r is also an unknown and is a function of the displacement, an iterative solution will be required. This, of course, is consistent with the non-linear characteristic of the problem.

Two numerical methods for calculating the deformed shape of the spring will be introduced. Theoretical results obtained using these two methods are then compared with test results of the experimental program.

Method 1: Numerical integration. This method uses the equations for the curvature, slope, and deflection of the spring. The values, ϕ, θ and y, are dependent upon the magnitude of the roller reaction force F_r, but F_r is conversely dependent upon L, the distance between the roller and the drum. Therefore an iterative solution based upon the roller reaction force will be necessary. If the deformed shape calculated using Equation 4 results in a drum-roller distance (L) that is equal to the actual drum-roller distance, then the solution is based upon the correct roller reaction force. The relation between L and the roller reaction force is shown in Figure 9. If the roller is close to the drum (i.e. L is small) the roller reaction force is large. If L is large, however, the roller reaction force approaches a minimum.

To calculate L, the position of the center of the drum must be determined. The position of the center of the drum is calculated by first determining the x and y coordinates of the tangent point B and the slope of the deflection curve at B. Since a radial of the drum will be perpendicular to the deflection curve at point B the position of the center of the drum can be calculated.

It should also be noted that it can be shown that the rotation required to develop the full strength of the spring (θ_p) is equal to the rotation to the tangent point B (Reference 2). This is the angle with vertex at the center of the drum, measured from the center of the roller to the tangent point B (see Figure 10).
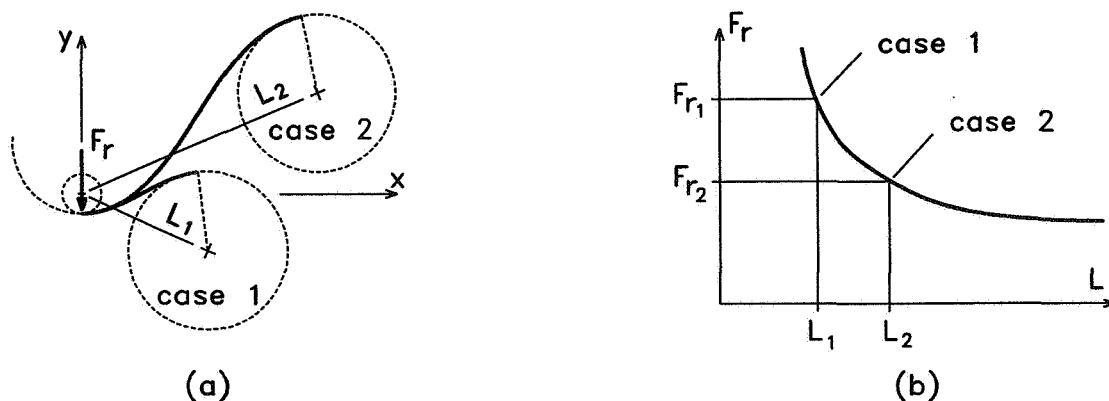

(a)   (b)

Figure 9. Relation Between the Roller Reaction Force F_r and L

The procedure for finding the correct solution can be summarized as follows:

* Assume a value for F_r.
* Use Equation 4 to calculate x_t.
* Use Equation 2 to calculate the slope of the deflection curve at point B.
* Solve for the y value of point B by numerically evaluating Equation 3.
* Now that the position and slope of the curve at point B have been determined, calculate the coordinates of the center of the drum.
* Calculate L and compare to the actual L.
* If the calculated value of L differs from the real value, adjust F_r accordingly and repeat until the value of F_r that corresponds to the real value of L is converged upon.
* Use true F_r to calculate deflection, rotation, or curvature for any point along the deflection curve. Since the position of point B and the center of the drum are known, the angle θ_p can also be calculated.

Method 2: Finite segments. The second method for calculating the deformed shape relies only upon the expression for the curvature (Equation 2). As in the first method a value of F_r is assumed. However, in this method the driving parameter is s, the distance measured along the deformed curve from point A. Recalling that the curvature is defined as the change in slope per unit length ($\phi = d\theta/ds$) the following scheme is used to calculate points along the deformed shape of the spring.

Initial values	Differential values	Updated values
$s = 0$	ds = small finite value	$s = s + ds$
$\theta = 0$	$d\theta = \phi ds$	$\theta = \theta + d\theta$
$x = 0$	$dx = ds\cos\theta$	$x = x + dx$
$y = -1/R_r$	$dy = ds\sin\theta$	$y = y + dy$
$\phi = \phi_n$		$\phi = \phi_n - F_r x/EI$

A value for the reaction force is assumed. Initial values corresponding with the actual restraint conditions at point A are set. These values are then updated using differential values for each additional segment ds along the curve. At some point along the curve the curvature will become equal to the curvature of the surface of the drum. This signifies that the spring is now tangent to the drum. The updated values at this point are for point B, the tangent point of the drum. The x, y, and slope values for that point are used to calculate the position of the center of the drum and the corresponding value of L. This calculated value of L is compared to the real value of L and then the assumed value of F_r is adjusted accordingly. This process is repeated until the correct solution is converged upon.

An AutoLISP algorithm which uses this method has been developed. This algorithm solves for the deflected shape of the spring and plots the spring, the drum, and the roller as an AutoCAD drawing file. Analytical results using this routine will be used in the comparison of the test results.

<u>Comparison with test results</u>. In solving for the displaced shape of the spring, several important characteristics of the spring have been revealed. Of particular interest are the following:

- The general shape of the spring
- The rotation required to develop the full strength of the spring θ_p
- The angle of contact between the spring and roller θ_t
- The tangent-to-tangent segment length s_t

These four characteristics will be used to compare the analytical solution with test results. These values vary for each unique combination of spring size and drum-roller configuration. Figure 10 illustrates qualitatively how each of these characteristics will vary just by changing the distance between the drum and roller.

The first characteristic to be addressed is the general shape of the spring. Figure 11 shows a photograph of the deformed shape of a typical spring in the loaded position. Superposed on the photograph is a plot of the analytical solution for the deformed shape of the spring. Figure 11 is still somewhat of a qualitative comparison, but it is important because it shows that space requirements can be checked analytically rather than by building a prototype to see if the deflected spring will have clearance problems.
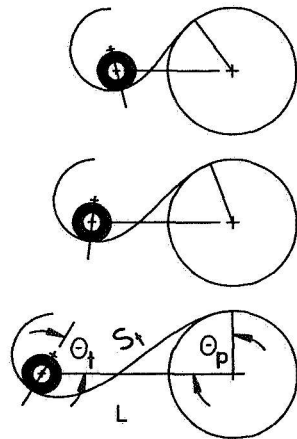

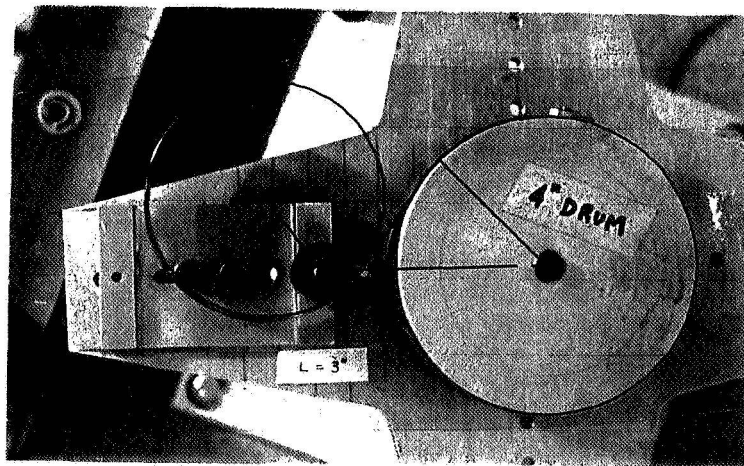**Figure 10. Variation in the Deflected Shape of the Spring**

Figure 11. Deformed Shape of a Spring

The next characteristic to be compared is the angle θ_p. This is the rotation at which the spring develops its full strength. θ_p varies for different spring sizes and drum-roller configurations. Even for a given spring, drum, and roller, θ_p will vary if the distance between the drum and roller is changed. Figure 12 shows torque-rotation curves for three different values of L using the same spring, drum, and roller. When L is small, in other words when the roller is close to the drum, it takes less rotation to develop the full torque of the spring than when L is large. θ_p can vary by as much as 90 degrees in some cases depending upon the distance between the drum and roller. Table 2

compares values of θ_p calculated using method 1 and method 2 with test results for a typical constant-torque spring configuration. Except for small values of L the calculated values are accurate to within 2 or 3 degrees. This is because, as illustrated in Figure 13, the slope of the curve is so steep that small errors in measuring L result in large errors for θ_p.
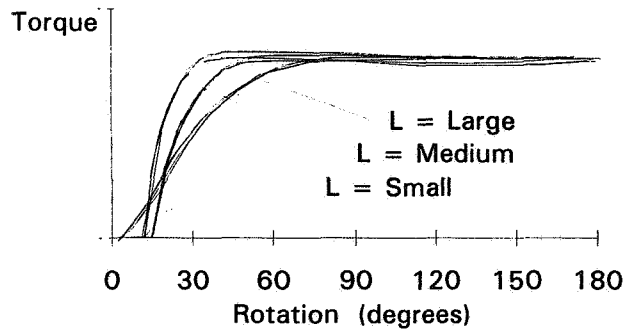
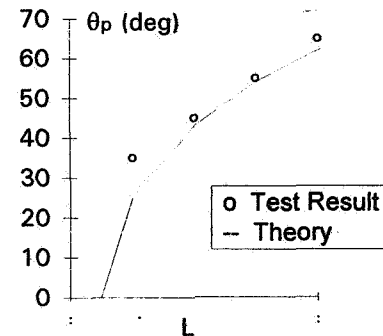Figure 12. Torque-Rotation Curves Illustrate the Variability of θ_p

Figure 13. θ_p, Comparison of Analysis with Test Results

The other characteristics of interest are the angle of contact between the spring and the roller (this angle is called θ_t and defines the orientation of the roller reaction force; see Figure 10), and the tangent to tangent segment length s_t. s_t is directly calculated when using the finite segment method, and can also be included in the calculation when using the numerical integration method.

Table 2 compares values calculated using method 1 and method 2 with test results for a typical constant-torque spring configuration. The results presented are for single layered springs but are also comparable to results for layered springs. The results of tests for multi-layered springs (Reference 2) demonstrate that the characteristics of the deflected shape of a layered spring do not significantly differ from the characteristics of the individual springs used to make the layered spring.

Table 2. Comparison of Test Results to Methods 1 and 2

L (mm)	θ_p (deg)			θ_t (deg)			s_t (mm)		
	Test Result	Method 1	Method 2	Test Result	Method 1	Method 2	Test Result	Method 1	Method 2
44	35	25	25	144	145	145	20	20	20
50	45	43	43	122	120	120	36	38	38
57	55	54	54	105	104	104	48	50	50
63	65	62	62	90	92	92	58	62	62
70	70	69	69	81	83	83	72	74	74

The Effects of Friction

There are two sources of friction that need to be considered: the friction in the roller and the inter-laminar friction between spring layers.

<u>Effects of friction in the roller.</u> First it is necessary to differentiate between the two types of rollers commonly used. There are rollers that rotate and there are rollers that are just a fixed shaft. The first type of roller rotates about its center and may make use of a journal bearing, a ball bearing or some other type of bearing. This type of roller will be called a "bearing roller". This is the typical roller shown in all the previous illustrations. The second type of roller is not an actual roller, but is a fixed post or shaft that cannot rotate. Using a fixed shaft in place of a roller is not uncommon; many constant torque-spring mechanisms are designed using simply a steel pin for a roller. This type of roller will be called a "sliding roller" because when the spring is loaded or unloaded the spring slides along the surface of the fixed pin or shaft. It should be noted that if the typical bearing type roller were to bind or "freeze up" it would become a sliding roller, too. So the behavior of the sliding roller is of interest regardless of the type of roller used. In the case of a sliding roller, friction occurs when the surface of the spring actually drags across the surface of the roller. In the case of a bearing roller friction occurs within the bearing and not between the spring and the roller.

It can be shown that the hysteresis e in the torque-rotation curve due to the effects of friction in the roller can be expressed using Equation 5 (Reference 2). Where R_d is the radius of the drum, F_r is the roller reaction force obtained analytically using the methods described in the previous sections, and f is the "coefficient of friction" of the roller.

$$e = f\, F_r\, 2\, R_d \qquad\qquad (5)$$

Test results for a wide variety of constant-torque spring configurations demonstrate that this relationship is indeed linear (Figures 14. and 15). In Figures 14 and 15 the slope of the lines represents the coefficient of friction of the roller f. For these plots e was measured and F_r was calculated.
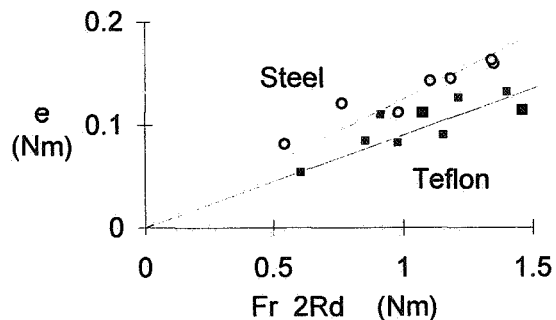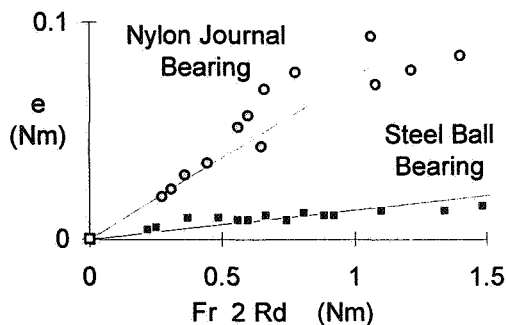

Figure 14. Bearing Rollers: e vs $F_r\, 2R_d$ Figure 15. Sliding Rollers: e vs $F_r\, 2R_d$

214

f can also be determined experimentally using the classical technique illustrated in Figure 16. In this method a length of spring coil is secured to a flat surface. Then the roller that will be used is placed on top of the spring. (If it is a bearing roller, the two axle configuration is used; if it is a sliding roller, the roller is oriented such that it will slide down the slope rather than roll.) The flat surface is then raised to the angle at which the forces of friction are overcome by the forces of gravity. The roller coefficient of friction is calculated using Equation 6. Table 3 compares values of *f* obtained using the sliding test with the slope of the e vs $F_r 2R_d$ curves shown in Figures 14 and 15.

Table 3. Predicting Values of *f*

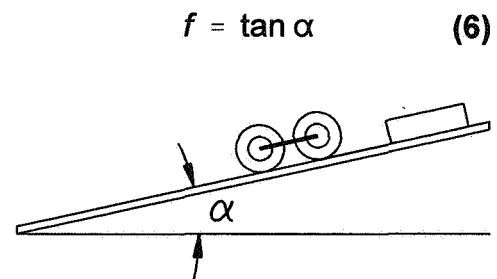|	Slope of e vs $F_r 2R_d$ line	Sliding Test
Steel Sliding Roller	0.12	0.14
Teflon Sliding Roller	0.09	0.09
Nylon Journal Bearing	0.13	0.14
Steel Ball bearing	0.013	0.02

$$f = \tan \alpha \qquad (6)$$

Figure 16. Testing for *f*

As the values of *f* get small (see steel ball bearing results) it becomes difficult to accurately measure e or predict *f* using the sliding test. Fortunately, for values of *f* this small the effect of friction on the torque-rotation curve is negligible.

The effects of friction between spring layers. Test results demonstrating the effects of friction between spring layers for a four-layered spring configuration made of type 301 stainless steel are shown in Figure 17. Torque-rotation curves for a one-, two-, three-, and four-layered spring are shown. With the addition of each succeeding spring layer
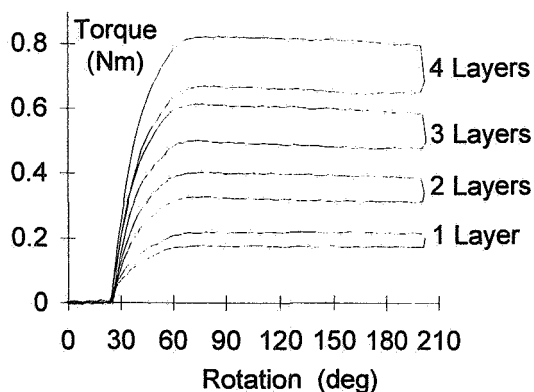
Figure 17. Torque-Rotation Curves for Multiple Layers of Springs

Table 4. Hysteresis by Spring Layer

Spring Combination	e (Nm) measured	$\sum$ e	%
Layer 1 only	.035	-	-
Layer 2 only	.036	-	-
Layer 3 only	.038	-	-
Layer 4 only	.038	-	-
Layers 1, 2	.071	.071	100%
Layers 1, 2, 3	.106	.109	97%
Layers 1, 2, 3, 4	.142	.147	97%

the magnitude of the hysteresis increases. This could lead to the conclusion that the increased hysteresis is related to the friction between each additional layer. However, it must be remembered that with the addition of each additional layer the roller reaction force also increases, and hence the hysteresis due to friction in the roller increases. In order to determine how much of the hysteresis is due to relative motion of the spring layers, the increased hysteresis due to the roller must first be subtracted out. The hysteresis of each individual spring and the hysteresis of multiple spring combinations are given in Table 4. By subtracting out the hysteresis due to the roller, we find that the remaining hysteresis due to relative sliding between spring layers was smaller than the accuracy of the test. Therefore, it is concluded that hysteresis due to relative sliding of spring layers is insignificantly small compared to the effects of friction in the roller.

Design Example

The following is a design example that incorporates the new analysis techniques. The design requirements shown in Table 6 will be used. Safety factors are examples and do not represent recommendations.

Table 6. Example Design Requirements

	Required Value	Safety Factor	Design Value
Torque Rotation Fatigue Life Operating Space	2.5 Nm (T_{REQ}) 180° (ϕ_{REQ}) 500 cycles 120 mm x 200 mm	4 $\phi_{LM} = 10°$, $\phi_{UM} = 10°$ 4 1	10 Nm (T_{DES}) 200° ($\phi_{LM} + \phi_{REQ} + \phi_{UM}$) 2,000 cycles 120 mm x 200 mm

Upper and Lower Margins of Safety for Rotation

Determine the spring material. Spring manufacturers can help in determining the appropriate spring material to be used. Type 301 stainless steel is the most common material used and will be selected for this example.

Determine the stress factor. Using a fatigue life curve such as the one shown in Figure 18, determine the stress factor S_f corresponding to the fatigue life design value. (Spring manufacturers can provide stress factors corresponding to the fatigue life of their specific products.) The stress factor is proportional to the cyclic stress range in the spring and is equal to the product of the thickness of the spring and the change in curvature the spring will experience (Equation 7). For the material used in this example the stress factor for 2,000 cycles is 0.0275.
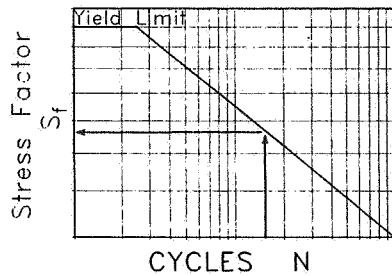
Figure 18. Fatigue Life Curve

$$S_f = t \left(\frac{1}{R_n} + \frac{1}{R_d} \right) \qquad (7)$$

Estimate the drum size. The drum must fit within the 120 mm operating space. Therefore, a drum diameter of 100 mm will be chosen; hence R_d = 50 mm. Minimizing the drum size can reduce the size and weight of the mechanism, so hopefully R_d can be reduced even more. But for starters we will use a diameter of 100 mm. In the case that there are no space requirements, use your best judgement to choose a "reasonable" drum diameter to start with.

Determine α, the ratio of drum diameter to spring diameter. Use the recommendations in Table 7 to select α (α = R_d/R_n). Most constant-torque spring design guides recommend that the drum diameter be twice the spring diameter (α = 2). However, in order to optimize mass and maximize rotation, this author recommends α = 1.25. α should never be less than 1.0 because instabilities can occur when the drum diameter is less than the spring diameter.

Table 7. Recommended Values of α

α	Achievable Rotation	Comments
Less than 1	-	Causes instability
1	270° ~ 300°	Achieves maximum rotation range
1.25	200° ~ 230°	Authors recommendation
1.5	150° ~ 180°	
1.75	115° ~ 145°	
2	90° ~ 120°	Commonly used
Greater than 2	less than 90°	Small rotation ranges

Determine the natural radius of the spring coil. Based upon α the natural radius of the spring coil is determined.

$$R_n = \frac{R_d}{\alpha} = \frac{50 \text{ mm}}{1.25} = 40 \text{ mm}$$

217

Calculate the maximum allowable spring thickness t_{max}.

$$t_{max} = \frac{S_f}{\left(1/R_n + 1/R_d \right)} = \frac{S_f\, R_d}{(\alpha + 1)} = \frac{(0.0275)\ (40\ mm)}{(1.25 + 1)} = 0.49\ mm$$

Select a spring. Select a spring with a thickness smaller than or equal to the maximum allowable thickness. If using stock springs, the catalog will give the width (b) of the spring and the initial diameter (ID) of the spring. The natural radius of stock springs must be modified to the design value if optimization of the mechanism is desired. If the spring is to be ordered to specifications, specify a thickness smaller than the maximum allowable thickness and specify a width approximately 60 to 100 times greater than the thickness (Reference 1). For this example the next standard thickness smaller than t_{max} is 0.4064 mm (0.016 in).

Determine the roller diameter. The roller diameter must be smaller than the spring ID. For this example a roller diameter of 25.4 mm will be used. 25.4 < 80, therefore, OK.

Determine the drum-to-roller distance L. The distance L influences the magnitude of θ_p, the magnitude of the roller reaction force F_r, and the inclination of the roller reaction force θ_t. In order to optimize mass, L should be small. However, if L is too small the magnitude of the roller reaction will increase, resulting in large hysteresis effects. Based upon results of the testing program the author recommends using a value of L that results in an angle of inclination of 110° for the roller reaction force. An analysis of the spring is carried out iteratively for various values of L until the one which results in $\theta_t = 110°$ is converged upon. Figure 19 shows the results of such a routine for this design example. Note how the appropriate value of L was selected so that θ_t would result in a value of 110°.

DRUM-ROLLER CONFIGURATION

Drum diameter	= 100
Roller diameter	= 25.4
Center-Center dist (L)	= 89.5

SPRING DATA

Thickness (t)	= 0.4064
Width (w)	= 25.4
Initial Diameter (ID)	= 80
Young's Modulus (E)	= 193,000

RESULTS OF ANALYSIS

Torque (T)	= 1388
Roller reaction force (F$_r$)	= 16.54 @ 110°
Tangent to tangent length (s$_i$)	= 81.8
Minimum rotation (θ_p)	= 59

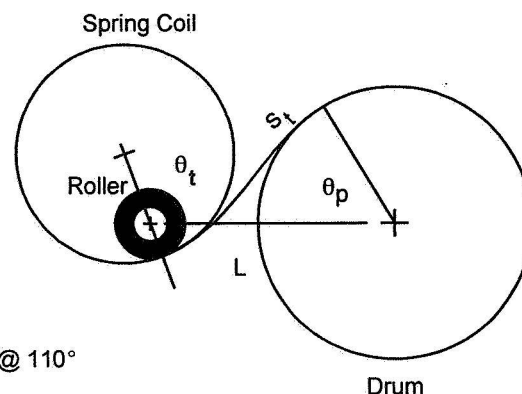Figure 19. Results of Analysis (Units: Newtons, Millimeters)

Calculate the constant-torque value T.

$$T = \frac{E\,b\,t^3}{24}\,R_d\left(\frac{1}{R_n} + \frac{1}{R_d}\right)^2$$

$$= \frac{(190{,}000\ \text{N mm}^2)\,(25.4\ \text{mm})\,(0.4063\ \text{mm})^3}{24}\,(50\ \text{mm})\left(\frac{1}{(40\ \text{mm})} + \frac{1}{(50\ \text{mm})}\right)^2$$

$$= 1{,}388\ \text{Nmm} = 1.388\ \text{Nm}$$

Calculate the magnitude of the hysteresis e. We will assume that a "sliding test" resulted in a roller coefficient of friction of 0.10.

$$e = f\,F_r\,2\,R_d = (0.1)\,(16.54\ \text{N})\,(50\ \text{mm}) = 82.7\ \text{N mm} = 0.0827\ \text{N m}$$

Calculate the effective torque for one layer T_{eff}. The effective torque is equal to the calculated torque less one half of the hysteresis. In this case the hysteresis resulted in a 3% loss of torque.

$$T_{eff} = T - \frac{e}{2} = 1.388\ \text{Nm} - \frac{0.0827\ \text{Nm}}{2} = 1.347\ \text{Nm}$$

Calculate the number of spring layers required n. Divide the design torque by the effective torque of one layer to determine how many spring layers are required. In order to optimize mass this author recommends using between 5 and 10 layers. If less than 5 layers are required, the drum can be made smaller and the analysis procedure repeated. If more than 10 layers are required, the drum should be made larger and the analysis procedure repeated. In the case that the drum cannot be made larger, more than 10 layers could be used, but tests to confirm stability should be performed.

$$n = \frac{T_{des}}{T_{eff}} = \frac{10\ \text{Nm}}{1.347\ \text{Nm}} = 7.4 \rightarrow 8\ \text{layers}$$

This design has 8 layers, and will therefore be accepted. The design could be fine tuned a bit by adjusting the drum diameter and repeating the procedure to this point, however, we shall accept this design and proceed.

Calculate the required length of the spring S. This calculation is for one spring layer.

$$S = s_t + R_d\left(\phi_{DES} \times \frac{\pi}{180}\right) = 81.8 + (50)\left(200° \times \frac{\pi}{180}\right) = 256\ \text{mm.}$$

<u>Calculate the maximum and minimum rotation values.</u> These are the rotation values between which the mechanism should operate.

$$\theta_{min} = \theta_p + \phi_{LM} \qquad = 59° + 10° \qquad = 69°$$

$$\theta_{max} = \theta_p + \phi_{LM} + \phi_{REQ} = 59° + 10° + 180° = 249°$$

This completes the proposed design procedure. The torque-rotation response of the spring is completely defined, the deflected shape of the spring is known, and all the important parameters required to specify the spring, drum, and roller have been determined. This design procedure, however, is only a recommendation, the analysis capabilities presented herein can, of course, be used to enhance other design procedures as needed.

Conclusion

In order to improve the design and analysis procedure of constant-torque springs used in aerospace applications several new analysis techniques were developed along with a design procedure which incorporates these new capabilities. The new analysis techniques include solutions for the deflected shaped of the spring, the roller reaction force, and the hysteresis effects of friction. Experimental results show that these new techniques are accurate and reliable, thus allowing several new aspects to be included in the design process.

The capacity to accurately calculate the deflected shape of the spring allows for space requirements and kinematic functionality of the spring mechanism to be checked analytically rather than using the time consuming process of trial and error.

References

1.   Votta, F. A. "The theory and design of long-deflection constant-force spring elements." <u>Transactions of the ASME</u>, (September, 1951). Vol 74.

2.   McGuire, J. <u>Analysis and Design of Constant-Torque Springs Used in Aerospace applications.</u> Ph.D. Dissertation, The University of Texas at Austin, December, 1994.

3.   Votta, F. A. "Constant-force springs for high output at short deflection." <u>Machine Design</u>, January 31, 1963. 102-106.